TITLE: QUANTIFYING THE INFLUENCE OF LOCAL METEOROLOGY ON AIR QUALITY USING GENERALIZED ADDITIVE MODELING

John L. Pearce[a*], Jason Beringer[a], Neville Nicholls[a], Rob J. Hyndman[b], and Nigel J. Tapper[a]

[a] School of Geography and Environmental Science, Monash University, Melbourne, Australia

[b] Department of Econometrics and Business Statistics, Monash University, Melbourne, Australia

Keywords: air pollution, climate change, generalized additive models, and meteorology.

*Corresponding author: School of Geography and Environmental Science, Monash University, Clayton, Victoria 3800. Tel: +61399054457. E-mail: john.pearce@monash.edu

ABSTRACT

This paper presents the estimated response of three pollutants, ozone (O_3), particulate matter ≤ 10 μm (PM_{10}), and nitrogen dioxide (NO_2), to individual local meteorological variables in Melbourne, Australia, over the period of 1999 to 2006. The meteorological-pollutant relationships have been assessed after controlling for long-term trends, seasonality, weekly emissions, spatial variation, and temporal persistence using the framework of generalized additive models (GAMs). We found that the aggregate impact of local meteorology in the models explained 26.3% of the variance in O_3, 21.1% in PM_{10}, and 26.7% in NO_2. The marginal effects for individual variables showed that extremely high temperatures (45 °C) resulted in the strongest positive response for all pollutants with a 150% increase above the mean for O_3 and PM_{10} and a 120% for NO_2. Other variables (boundary layer height, winds, water vapor pressure, radiation, precipitation, and mean sea-level pressure) displayed some importance for one or more of the pollutants, but their impact in the models was less pronounced. Overall, this analysis presents a solid foundation for understanding the importance of local meteorology as a driver of regional air pollution in Melbourne in a framework that can be applied in other regions. This paper presents an improved display method where the effects across the range of the covariate on each pollutant were quantified on a percentage scale. Such presentation facilitates easy interpretation across covariates and models. Finally, our results provide a clear window into how potential climate change may affect air quality.

1. Introduction

It is well known that concentrations of gases and aerosol particles within local air sheds are affected by weather (Elminir 2005; Beaver and Palazoglu 2009). This understanding has led the air quality community to recognize that air pollution is an area sensitive to potential climate change. In an effort to provide those responsible for air quality management with potential 'what if' scenarios, a growing body of research on assessing the impacts of a changing climate on regional air quality has developed (Jacob and Winner 2009; USEPA 2009). This increased scrutiny of air quality has highlighted that there are many aspects of air pollution that are still difficult to understand. One of these aspects is the estimation of the sensitivity of air pollutants to individual meteorological parameters. This has proven particularly challenging for several reasons (USEPA 2009). First, meteorological parameters are inherently linked, resulting in strong interdependencies, for example, the dependency of boundary layer height on surface temperature or the link between surface temperature and radiation. These associations make separating the effects of individual parameters a highly complex task. Secondly, meteorological parameters can affect pollutants through direct physical mechanisms such as the relationship with radiation and ozone or indirectly through influences on other meteorological parameters such as the association between high temperatures and low wind speed (Jacob and Winner 2009). Thus, multiple approaches are necessary to understand the true nature of meteorological-pollutant relationships. To further complicate matters, the magnitude and nature of these effects can vary from one air shed to the next as well as across seasons, making site specific assessments necessary for understanding local responses (Dawson, Adams et al. 2007a; USEPA 2009).

Statistical modeling is one approach that can be used for addressing the effects of meteorology on air pollution (Camalier, Cox et al. 2007). Statistical models are well suited for quantifying and visualizing the nature of pollutant response to individual meteorological

parameters as they directly fit to the patterns that arise from the observed data (Schlink, Herbarth et al. 2006). However, statistical techniques do not aim to fully describe the formation and accumulation of air pollutants in their chemical, physical, and meteorological processes (Schlink, Herbarth et al. 2006). In order to obtain a robust understanding for these aspects of air quality a combined approach including deterministic models is suggested (Jacob and Winner 2009). That being said, statistical modeling is a widely used, effective learning tool for a variety of air quality applications (Thompson, Reynolds et al. 2001; Schlink, Herbarth et al. 2006). Furthermore, non-linear statistical approaches have been shown to effectively describe the complex relationship between meteorological variables and air pollution (Thompson, Reynolds et al. 2001). Unfortunately, summarizing non-linear associations beyond a graphical display has often proved difficult and provided little information that is interpretable to the general public (Thompson, Reynolds et al. 2001). In the context of climate change impacts on air quality it has been suggested that statistical studies are most capable of providing insight into the potential impacts through development of observational foundations (Jacob and Winner 2009). These foundations provide a window into the possible extent of climate change impacts on air quality (Camalier, Cox et al. 2007).

This study aims to provide such an observational description for Melbourne, Australia. The city of Melbourne, with a population of approximately 3.9 million (ABS 2010), is situated on Port Phillip Bay at the south-eastern edge of the continent in close proximity to the Southern Ocean at 37° 48’ 49” S 144° 57 47” E (Figure 1). The climate can best be described as moderate oceanic, with occasional incursions of intense heat from Central Australia, and the city is famous for its highly changeable weather conditions (BOM 2009). Locals like to declare that Melbourne weather typically observes ‘four seasons in one day’. While Melbourne’s air pollutant levels are relatively low (Table 1) when compared to other urban centers of similar size, the city is subjected to a wide range of meteorological

conditions that present an interesting opportunity for analysis (Murphy and Timbal 2008). With increasing population growth and urbanization in the Melbourne region there will be added pressures on air quality, which may result in less favorable conditions in the future. This will be superimposed upon the predicted effects of climate change.

The objective of this research is to quantify the magnitude in which regional air pollutants respond to local meteorology in Melbourne, Australia. This was achieved using the framework of generalized additive modeling (GAM) to estimate the response of ozone (O_3), particulate matter $\leq$ 10 μm (PM_{10}), and nitrogen dioxide (NO_2) to individual local meteorological variables. The meteorological-pollutant relationships have been assessed after controlling for long-term trends, seasonality, weekly emissions, spatial variation, and temporal persistence. The nature of the response of each pollutant to individual meteorological variables is presented using partial residual plots described on a percentage scale as marginal effects.

2. Data

a. Local Meteorological Data

Links between air pollutants and local weather conditions were made using daily automatic weather station observations for site number 086282 (Melbourne International Airport) for the period of 1999 to 2006. This site is located at 37° 40’ 12” S and 144° 49’ 48” E with an elevation of 113 m and was chosen because a comprehensive range of measures are collected consistently over time. Variables provided by the Australian Bureau of Meteorology included:

- Maximum daily temperature (°C)
- Mean sea-level pressure (hPa)
- Global radiation (MJ/m^2)
- Water vapor pressure (hPa)

- Zonal (*u*) and meridional (*v*) wind components (km/hr)
- Precipitation (mm).

Additionally, boundary layer height (BLH) was taken from the ERA-Interim reanalysis using the location of 37° 30' 0" S and 145° 30' 0" E for 4 p.m. LST - the approximate time of maximum boundary layer depth. The ERA-Interim reanalysis is produced by the European Centre for Medium-Range Weather Forecasts (ECMWF) and is discussed in more detail by Uppala, Dee et al. (2008).

b. Air Pollutant Monitoring Data

Local air pollution data were provided by the Environmental Protection Authority Victoria taken from the Port Phillip Bay air monitoring network (Figure 1). Pollutants included ozone (O_3), particulate matter ≤ 10 μg (PM_{10}), and nitrogen dioxide (NO_2). O_3 and NO_2 concentrations are reported in parts per billion by volume (ppb) and were measured using pulsed fluorescence chemiluminescence and ultra violet absorption techniques. PM_{10} concentrations were measured using photospectrometry and are reported in micrograms per cubic meter ($\mu g/m^3$). This analysis uses the daily maximum value for 8-hr O_3, the 24-hr mean value of PM_{10}, and the daily maximum value for 1-hr NO_2 from all available monitoring locations over the period of 1999 to 2006 (Table 1). These timeframes were selected to parallel air quality objectives in the State Environment Protection Policy for ambient air quality (SEPP 1999). Additionally, days on which significant air quality events (bushfires, dust storms, factory emissions, etc.) were known to have occurred and data below 5 ppb for O_3 and NO_2 and 3 $\mu g/m^3$for PM_{10} were removed.

3. Methods

a. Generalized Additive Modeling

Generalized additive models (GAMs) are regression models where smoothing splines are used instead of linear coefficients for covariates (Hastie and Tibshirani 1990). This approach

has been found particularly effective at handling the complex non-linearity associated with air pollution research (Dominici, McDermott et al. 2002; Schlink, Herbarth et al. 2006; Carslaw, Beevers et al. 2007). The additive model in the context of a concentration time series can be written in the form (Hastie and Tibshirani 1990):

$$log(y_i) = \beta_0 + \sum_{j=1}^{n} s_j(x_{ij}) + \varepsilon_i \quad (3.1)$$

where y_i is the ith air pollution concentration, β_0 is the overall mean of the response, $s_j(x_{ij})$ is the smooth function of ith value of covariate j, n is the total number of covariates, and ε_i is the ith residual with var(ε_i)= σ^2, which is assumed to be normally distributed. Smooth functions are developed through a combination of model selection and automatic smoothing parameter selection using penalized regression splines, which optimize the fit and make an effort to minimize the number of dimensions in the model (Wood 2006). Interaction terms, e.g. $s(x_1, x_2)$, can also be modeled as thin-plate regression splines or tensor product smooths. The choice of the smoothing parameters is made through restricted maximum likelihood (REML) and confidence intervals are estimated using an unconditional Bayesian method (Wood 2006). This analysis was conducted using the *gam* modeling function in the R environment for statistical computing (R Development Core Team 2009) with the package 'mgcv' (Wood 2006).

c. Model Development

The first step in the selection of individual models for O_3, PM_{10}, and NO_2 was to fit a preliminary base model. This was fit to each pollutant in order to control for the seasonality, persistence, spatial trend, and weekly emissions patterns that exist in these data. Following model (3.1) the preliminary model can be written as:

$$\log(y_i) = \beta_0 + s(time) + s(dow) + s(long, lat) + s(y_{i-1}) + \varepsilon_i \quad (3.2)$$

where *time* is a number between 1 and 2922 included to account for long-term trends and seasonality, *dow* is a number ranging from 0 to 6 included to account for day-of-the-week, *long* and *lat* are the spatial coordinates of each monitor location included to account for spatial trend, and y_{i-1} is a one day lag term included to account for short-term temporal persistence. It is important to note that the residual spatial variation is controlled by including a tensor product smooth, $s(long, lat)$, in the model and a smooth function of the preceding day's pollutant concentration, $s(y_{i-1})$, was included to control for autocorrelation in residuals. Additionally, since air pollution data are known to be seasonal, a predetermined smoothing parameter of k=32 (one knot (k) for each of the four seasons over the study period) was used for the construction of the spline function for *time*. The motivation for this control is that function should represent a relatively symmetric cyclic pattern in the data. To check the adequacy of our methods for controlling for space-time effects, box-plots and time-series plots of residuals by monitor location were examined. No violations of assumptions were obvious in any pollutant.

Final models were chosen using forward selection where each of the meteorological variables was added to the base model upon which Akaike's Information Criteria (AIC) was evaluated. A variable remained in the final model if the fit yielded a lower AIC. Following model (3.1), the final model for each pollutant that can be written as:

$$\log(y_i) = \beta_0 + s(time) + s(dow) + s(long, lat) + s(y_{i-1}) + s(temp) + s(u) + s(v) + s(wvp) + s(rad) + s(precip) + s(blh) + \varepsilon_i \quad (3.3)$$

where *temp* is daily maximum temperature, u is the zonal wind component, v is the meridional wind component, *wvp* is water vapor pressure, *rad* is radiation, *precip* is precipitation and *blh* is the 4 p.m. boundary layer height. It is important to note that

exploratory analysis included covariates not listed in Table 1. This included using winds over shorter periods, various measures of radiation, temperature, and atmospheric moisture. None of these refinements made any significant improvements to the models.

e. Characterization of Meteorological Effects

The explanatory powers of the final models specified above were measured using the R^2 statistic. The aggregate impacts of local meteorology on each pollutant are assessed by the difference in the R^2 of model (3.2) and model (3.3). Individual relationships between particular meteorological variables and each air pollutant are assessed using partial response plots.

It is well known that representing the full relationship between the response and the predictor in multiple regression models is difficult due to high dimensionality (Faraway 2005). Therefore we opted to use partial response plots to reveal the marginal relationship between each meteorological variable and each air pollutant (Faraway 2005). A partial response plot shows the static effect (i.e. effects that are stable over time) of a particular meteorological variable on a particular pollutant after accounting for the effects of all other explanatory variables in the model (Camalier, Cox et al. 2007). This effect is described as the marginal relationship between the response and the predictor because it represents the relationship after the effects of all other predictors have been removed from the data (Faraway 2005). In our case, the *y*-axis of each partial response plot has been centered to the mean value of the response and adjusted to a percentage scale. These proportional values are the marginal effects (Harrell 2001). The marginal effect can be interpreted as the change in pollutant response from the mean as the covariate of interest is varied. In short, the partial regression plot allows us to focus on the relationship between one predictor and the response in isolation from the effects of other predictors in the model (Faraway 2005). Representing the marginal effects as proportions scaled to the mean make it easy to compare effects across

covariates and pollutants. The displayed marginal effects are given by $100 * [\exp(s(x))-1]$, where x is the meteorological variable of interest, and $s(x)$ is the corresponding smooth function in model (3.3).

4. Results and Discussion

a. Ozone

Ground-level ozone is classified as a secondary pollutant because it forms in the atmosphere when emissions of precursors such as volatile organic compounds (VOCs) and nitrous oxides (NO_x) react with sunlight (WHO 2006). Concentrations have been linked to atmospheric conditions such as the availability of solar ultraviolet radiation capable of initiating photolysis reactions, air temperatures, and concentrations of chemical precursors (USEPA 2009). Research conducted across many settings suggests that increasing O_3 pollution is most strongly linked with increases in temperature (Jacob and Winner 2009).

In Melbourne we found that model (3.3) explained 69.9% of the variance of log transformed O_3 with the components of model (3.2) accounting for 43.6% and the aggregate impact of meteorological variables accounting for 26.3%. The most significant meteorological variable for O_3 was temperature ($F=462.9$, $p<0.001$) with increased temperature being associated with increased ozone. This finding is most likely due to the role of temperature in the physical processes associated with ozone and its influence on local meteorology that affects air pollution. A partial residual plot (Figure 2) identified a positive non-linear relationship with marginal effects as great as 150%. This finding is in strong agreement with results from previous studies as increased temperatures have been shown to result in increased ozone in a variety of settings (Elminir 2005; Dawson, Adams et al. 2007a; Jacob and Winner 2009). A key finding here was that ozone concentrations were estimated to be 75-150% higher than average during the 92 days (3.5%) in the study period when daily maximum temperatures were in the range of 35 to 45 °C.

Water vapor pressure (F=27.5, p<0.001) was found to have little influence on ozone except when at the upper and lower extremes (Figure 2). Notably, increases of up to 80% were seen when water vapor pressure rose above 20 hPa. This positive response at high water vapor pressure is contradictory to findings that suggest that an increase in humidity suppresses ozone formation (USEPA 2009). With the exception of the strong positive relationships at high water vapor pressures, similar results were noted by Wise and Comrie (2005) for the dry climate of the south-western U.S. The estimated response for the zonal (u) wind component (F=5.6, p<0.001) in the model identified that increases up to 5% were expected when strong winds originated from the west and decreased with winds originating from the east. The response of ozone to meridional (v) wind (F=20.6, p<0.001) increased up to 15% under strong northerlies and decreased with winds from the south. The increase under north-west winds may be a result of inhibited local dispersion associated with a blocking of the bay breeze (Hurley, Manins et al. 2003). Weak winds have been associated with increased O_3 elsewhere (Dawson, Adams et al. 2007a). The effect of radiation (F=76.5, p<0.001) was found to be the strongest after values surpassed 20 MJ/m^2 as concentrations increased by as much as 25% (Figure 2). This relationship is consistent with the literature as radiation is a known driver in the photochemistry of ozone production (Dawson, Adams et al. 2007a). The response for mean sea-level pressure (MSLP) (F=27.5, p<0.001) found a slight increase in the marginal effects under low pressure (10%) and under moderate pressure (5%). The response was quite weak and is in relative agreement with other studies were MSLP has been found insignificant (Davis and Speckman 1999). The response of ozone to changes in boundary layer height (F=122.8, p<0.001) was found to be negative for heights below one kilometer where ozone decreased up to 40% (Figure 2). This negative effect is presumably due to an association with cold fronts that introduce clean air from the Southern Ocean into the Melbourne air shed. However, slight increases of up to 10% were shown between heights

of one to three kilometers. The moderate relationship observed in Melbourne agrees well with findings from other empirical studies where the role of mixing depth has been shown to be rather limited (Jacob and Winner 2009). The response of ozone to precipitation ($F=38.5$, $p<0.001$) showed increases of up to 40% as precipitation levels were at or below 40 mm (Figure 2). After this threshold, confidence intervals increase in size and the relationship was generally negative. This is presumably due to wet deposition during heavy rainfall. The positive effect during light rainfall has been noted elsewhere and suggests that some degree of atmospheric moisture is beneficial to ozone production (Ordonez, Mathis et al. 2005; Dawson, Adams et al. 2007).

Overall, the strongest positive response for O_3 was found for high temperature with a maximum increase of 150%. Interestingly, this was followed by an 80% increase under extremely high water vapor pressure. More research is suggested to identify the mechanism behind this response. The strongest negative response occurred under low boundary layer heights where concentrations were found to decrease by as much as 40% below average.

b. Particulate Matter

Particulate matter consists of solid or liquid particles found in the air, including dust, pollens, soot, and aerosols from combustion activities (WHO 2006). Particles originate from a variety of mobile, stationary, and natural sources, and their chemical and physical compositions vary widely. Furthermore, PM can be emitted directly or can be formed in the atmosphere when gaseous pollutants such as SO_2 and NO_x undergo transformation to form secondary organic particles. This complexity has been highlighted in studies showing that the chemical and physical composition of PM varies depending on location, source, time of year, and meteorology (USEPA 2009). A review of current research by Jacob and Winner (2009) found that observed correlations of PM concentrations with meteorological variables have been found to be inconsistent (direction depends on composition) and are generally weaker

than for ozone. This indicates that the relationship with particulate matter is more complicated than with gaseous pollutants and that dependencies are likely to vary from one air shed to the next.

In Melbourne we found that model (3.3) explained approximately 57.8% of the variance of log transformed PM_{10} with the components of model (3.2) accounting for 36.7% and the aggregate impact of meteorological variables accounting for 21.1%. Daily maximum temperature (F=265.6, p<0.001) was identified as the most significant meteorological variable and increasing temperatures corresponded with increasing PM_{10} (Figure 3). The nature of the response was similar to the findings for ozone (particularly when a threshold of 35 °C was surpassed) as resulting concentrations were 100 to 150% higher than average. It is important to note that this finding contradicts results from model perturbation studies (Dawson, Adams et al. 2007b). However, some North American studies have stated that a positive response may be driven by increases in the sulfate component or black carbon of PM due to faster SO_2 oxidation (Jacob and Winner 2009). This seems unlikely to be the case in Melbourne as research has found that PM in Australian cities is of very low sulfur content (Chan, Cohen et al. 2008). More research is suggested in order to identify the mechanism behind this response. Water vapor pressure was also found to be quite significant (F=143.4, p<0.001) where increases as great as 30% were seen when values dropped below 10 hPa (Figure 3). This finding is similar to findings in other areas where crustal/soil dust is an important source of regional PM (Wise and Comrie 2005). The response of PM_{10} to the zonal (u) wind component (F=34.1, p<0.001) indicated that under strong westerly winds concentrations increased by up to 20%. Meridional (v) wind (F=139.4, p<0.001) was also found to be quite significant with a 20% decrease occurring under strong northerly winds (Figure 3). The increase of PM_{10} under strong westerlies is most likely due to an increased contribution of regional dust and the decrease observed under strong northerlies is most likely

the result of increased dispersion. Furthermore, slight increases also occurred under relatively light to stable winds showing that transport related PM can buildup in the region. Other studies have noted the positive effect of stable conditions on PM in urban environments (Jacob and Winner 2009). Particles slightly increased (5%) under low levels of radiation ($F=34.6$, $p<0.001$) that suggests increases during periods of increased cloudiness and cooler months. The effect of mean sea-level pressure ($F=19.9$, $p<0.001$) shows that low pressures result in decreases up to 5% while increases of up to 10% were seen as pressures rose above 1020 hPa. This is most likely due to the strong association of high pressure with stability (USEPA 2009). The nature of the response of PM_{10} to the 4 p.m. boundary layer height ($F=22.6$, $p<0.001$) showed a 30% increase for heights below one kilometer and a decrease above this height. Dawson, Adams et al. (2007b) also noted a similar response for low boundary layer heights stating that decreased dispersion was a likely factor. Increased precipitation ($F=25.6$, $p<0.001$) was found to have a negative effect on particle concentrations (Figure 3). This finding is in agreement with other work since the role of precipitation in wet deposition is well known (Dawson, Adams et al. 2007b; Jacob and Winner 2009).

Overall, the strongest positive response of PM_{10}, like O_3, was under high daily maximum temperatures as concentrations were up to 150% higher than average. The second largest increase (30%) was under low boundary layer heights. The largest decreases were associated with increased precipitation (60%) and increased water vapor pressure (40%). Relatively stable winds had a much lesser effect than anticipated indicating that dust is likely a major source of particles for the region.

c. Nitrogen Dioxide

Nitrogen dioxide is a reddish brown toxic gas that forms when nitric oxide emissions from automobiles and power plants react with oxygen in the atmosphere (WHO 2006). In the

urban environment levels of NO_2 have been found to be strongly associated with emissions from vehicles and have also been found to contribute to the secondary formation of O_3 and fine particle pollution (USEPA 2009). While less research has focused on the meteorological links for NO_2 it has been found that local dispersion and temperature play important roles (Carslaw, Beevers et al. 2007).

In this study we found that model (3.3) explained 56.3% of the variance of log transformed NO_2 with the components of model (3.2) accounting for 29.6% and the aggregate impact of meteorological variables in the model accounting for 26.7%. Increases in daily maximum temperature ($F=227.7$, $p<0.001$) were found to correspond with increases in NO_2 (Figure 4). Temperatures below 20 °C resulted in a 20% decrease and temperatures above 40°C resulted in a maximum increase of 120%. This finding agrees with results from a single site in a multiple site study in Oslo, Norway, where a positive response was noted for temperatures across the range of 5 to 25 °C (Aldrin and Haff 2005). This may be partially explained by the influence of temperature on evaporative emission rates or the association between temperatures and other meteorological variables important to NO_2. Further research using deterministic models is suggested. The response of NO_2 to water vapor pressure ($F=77.7$, $p<0.001$) was similar in nature to the response for PM_{10} as increases up to 20% were shown for pressures below 10 hPa. As water vapor pressure increased above 10 hPa concentrations exhibited decreases. The small effect of relative humidity seen here was also noted by Aldrin and Haff (2005) and suggests that atmospheric moisture had relatively little influence on NO_2. The response of NO_2 to the zonal (u) wind ($F=150.7$, $p<0.001$) showed up to a 40% decrease under strong westerly winds and a slight increase under stable conditions (Figure 4). Meridional (v) winds ($F=589.1$, $p<0.001$) were found to be the most significant meteorological variable in the model with the response showing a 60% decrease under strong winds (Figure 4). An increase of up to 20% was shown for conditions that were stable.

Stable conditions likely result in the buildup of local emissions within the Melbourne air shed as Carslaw, Beevers et al. (2007) also noted wind as the most significant meteorological predictor for traffic related NO_2. The response to radiation ($F=50.8$, $p<0.001$) exhibited a modest negative relationship where high levels resulted in a regional decrease of up to 20% (Figure 4). Low mean sea-level pressure ($F=20.4$, $p<0.001$) resulted in up to a 10% decrease while high pressure showed up to a 10% increase. This is most likely explained by increased stability during periods of high pressure. The response to the 4 p.m. boundary layer height ($F=9.3$, $p<0.001$) showed that concentrations decreased up to 30% as the boundary layer rose (Figure 4). Increased dilution within the boundary layer is the likely mechanism. A positive response to light precipitation ($F=10.9$, $p<0.001$) was identified although it should be interpreted cautiously as confidence intervals are rather large.

Overall, the strongest positive response for NO_2 occurred under high temperatures when concentrations increased by as much as 120%. This was followed by precipitation although confidence intervals are quite broad likely due to a low frequency of occurrence. The largest decrease in concentrations was shown for *u* and *v* wind components as strong winds resulted in a 60% decrease below the mean. Water vapor pressure also had a negative effect as increased values resulted in a decrease of up to 40%. The degree to which NO_2 responded to local meteorology – particularly temperature and wind, was greater than expected. The findings here suggest that local meteorology is of the same magnitude of importance for NO_2 as it is for O_3 and PM_{10} in the Melbourne air shed.

d. Technical Approach

The use of GAM in combination with partial residual plots and marginal effects proved an effective and insightful way to characterize the relationships between individual meteorological variables representing local weather and air pollution. Complex non-linear dependencies were not only able to be visualized for each response, but their effects across

the range of the covariate were also able to be quantified on a percentage scale. This quantification provides an expansion upon previous analysis by facilitating easy interpretation across covariates and models, which is especially important for communicating results to non-specialized audiences. Although our approach did not consider the physical, meteorological and chemical processes in detail, the results produced were plausible and comparable to other studies. Furthermore, results produced are based on observational data eliminating the uncertainty associated with interpreting responses based on forecasts.

Perhaps the greatest limitation of the current work is the omission of interaction terms (ex. s ($temp$, v)) in the models. Not including these terms may have resulted in the underestimation of the overall impact of local meteorology on air pollution. However, it could also be stated that due to the interdependency of meteorological variables, interactions may be accounted for by a single dominant variable. In our case, this variable is most likely temperature. GAMs are quite capable of handling complex interactions and further research of models that include interactions is suggested. Minor improvements in this approach might include improved spatial resolution of all meteorological data as conditions in this paper are treated as being spatially uniform. Unfortunately, other locations throughout Melbourne did not contain a complete record for all variables of interest for our study period. This may have led to the misspecification of meteorology resulting in model errors even at times when conditions were conducive for increased air pollutant levels. Additionally, the inclusion of more sophisticated emissions data would likely improve model fit and therefore result in more accurate assessments of meteorological variables.

e. Potential Impacts of Climate Change

The Australian Greenhouse Office, using climate change projections developed by the Australian Bureau of Meteorology and the Australian Commonwealth Scientific and Research Organisation (CSIRO) for the city of Melbourne, anticipates a future air

environment that exhibits increased temperatures, decreased moisture, and decreased wind speeds (CSIRO 2007). Notably, a projected increase in the number of days above 35 °C on the magnitude of 25% (~3 days) by 2030 and 50-100% (~7-14 days) by 2070 is also expected (CSIRO 2007). If such projections hold true, this study provides evidence from observational data that the on the basis of the current level of emissions the air environment in Melbourne will become more conducive to poorer air quality. Our results confirm a statistically significant association between increasing pollutant concentrations and increasing temperatures. Therefore, it appears that increasing temperatures, particularly across the range of 35 to 45°C, will cause increases on the magnitude of 150% for O_3 and PM_{10} and 120% for NO_2, assuming everything else remains equal. Relationships with wind indicate that if increased periods of stability occur in the future then increases of 10 to 20% in PM_{10} and NO_2 are likely to occur and if increased winds from the northwest occur then increases up to 15% in O_3 will likely result. It is important to note that this finding is representative of the overall regional response to wind, not individual monitor's response to local winds. Findings for water vapor indicate that if the future climate brings increasingly drier conditions, then PM_{10} and NO_2 are likely to increase by as much as 25%. Our findings for radiation suggest that periods of increased cloudiness would likely result in slight increases of up to 5% for PM_{10} and NO_2 while the opposite can be said for O_3 which could see reductions up to 5%. If precipitation decreases in the future then increases will likely be seen for PM_{10} and NO_2. Changes in mean sea-level pressure (at the local scale) are not likely to significantly impact any pollutant. These findings provide an observational window into how climate change may affect local air quality in Melbourne through changes in local meteorology, but further research using synergistic processed base air quality models is suggested.

5. Conclusion

The overall objective of this study was to develop observational relationships between locally measured individual meteorological variables and select air pollutants in Melbourne, Australia. Moreover, a statistical methodology is presented for achieving this objective and results are presented in a manner where the complexities of those relationships are easily compared and understood. In Melbourne we found that local meteorological conditions most strongly affect the daily variation associated with O_3 and NO_2 followed closely by PM_{10}. The strongest effects for O_3 were related to temperature, boundary layer height, and radiation. The most significant variables for PM_{10} were temperature, wind, water vapor pressure, and boundary layer height. Temperature also displayed the strongest influence on NO_2 which was followed by wind and water vapor pressure. The remaining variables displayed some effect for each air pollutant, but the responses for these were less pronounced. These results can be used to determine the relative importance of local weather as a driver of regional air pollution as well as the marginal effects of individual meteorological variables. Furthermore, by presenting the percent change in air pollutant response across the range of individual meteorological variables, a clear window into how potential climate change may affect air quality is provided. This window suggests that a significant 'climate penalty' may need to be taken into account in order to achieve future air quality objectives.

Acknowledgements. The authors are grateful to Sean Walsh and Petteri Uotila for their important contributions to the data used in this study. This study was supported through research funds provided by the Environmental Protection Authority Victoria and Monash University. Neville Nicholls involvement was supported by the Australian Research Council through Discovery Project DP0877417.

TABLE AND FIGURE HEADINGS

Table 1. Summary of data used for model development.

Figure 1. Map of monitoring locations used in this study.

Figure 2. Partial response plots for O_3. The *y*-axis represents the marginal effects. The dashed lines are estimated 95% confidence intervals and the vertical lines adjacent to the lower *x*-axis represent the frequency of the data.

Figure 3. Partial response plots for PM_{10}. The *y*-axis represents the marginal effects. The dashed lines are estimated 95% confidence intervals and the vertical lines adjacent to the lower *x*-axis represent the frequency of the data.

Figure 4. Partial response plots for NO_2. The *y*-axis represents the marginal effects. The dashed lines are estimated 95% confidence intervals and the vertical lines adjacent to the lower *x*-axis represent the frequency of the data.

References

ABS (2010). Regional Population Growth, Australia 2007-2008, Australian Bureau of Statistics.

Aldrin, M. and I. H. Haff (2005). "Generalised additive modelling of air pollution, traffic volume and meteorology." Atmospheric Environment 39(11): 2145-2155.

Beaver, S. and A. Palazoglu (2009). "Influence of synoptic and mesoscale meteorology on ozone pollution potential for San Joaquin Valley of California." Atmospheric Environment 43(10): 1779-1788.

BOM. (2009). "Climate Statistics for Australian Locations." Retrieved 5 August, 2009, from http://www.bom.gov.au/climate/averages/tables/cw_086071.shtml.

Camalier, L., W. Cox, et al. (2007). "The effects of meteorology on ozone in urban areas and their use in assessing ozone trends." Atmospheric Environment 41(33): 7127-7137.

Carslaw, D. C., S. D. Beevers, et al. (2007). "Modelling and assessing trends in traffic-related emissions using a generalised additive modelling approach." Atmospheric Environment 41(26): 5289-5299.

Chan, Y. C., D. D. Cohen, et al. (2008). "Apportionment of sources of fine and coarse particles in four major Australian cities by positive matrix factorisation." Atmospheric Environment 42(2): 374-389.

Davis, J. M. and P. Speckman (1999). "A model for predicting maximum and 8 h average ozone in Houston." Atmospheric Environment 33(16): 2487-2500.

Dawson, J. P., P. J. Adams, et al. (2007a). "Sensitivity of ozone to summertime climate in the eastern USA: A modeling case study." Atmospheric Environment 41(7): 1494-1511.

Dawson, J. P., P. J. Adams, et al. (2007b). "Sensitivity of PM2.5 to climate in the Eastern US: a modeling case study." Atmospheric Chemistry and Physics 7(16): 4295-4309.

Dominici, F., A. McDermott, et al. (2002). "On the use of generalized additive models in time-series studies of air pollution and health." American Journal of Epidemiology 156(3): 193-203.

Elminir, H. K. (2005). "Dependence of urban air pollutants on meteorology." Science of the Total Environment 350(1-3): 225-237.

Faraway, J.J. (2005). Linear models with R. Boca Rotan, Florida,Chapman and Hall.

Harrell, F. E. (2001). Regression modeling strategies: with applications to linear models, logistic regression, and survival analysis. New York; London, Springer.

Hastie, T. J. and R. J. Tibshirani (1990). Generalized Additive Models. London, Chapman & Hall.

Hurley, P., P. Manins, et al. (2003). "Year-long, high-resolution, urban airshed modelling: verification of TAPM predictions of smog and particles in Melbourne, Australia." Atmospheric Environment 37(14): 1899-1910.

Jacob, D. J. and D. A. Winner (2009). "Effect of climate change on air quality." Atmospheric Environment 43(1): 51-63.

Murphy, B. F. and B. Timbal (2008). "A review of recent climate variability and climate change in southeastern Australia." International Journal of Climatology 28(7): 859-879.

R Development Core Team (2009). R: A language and environment for statistical computing. Vienna, Austria, R Foundation for Statistical Computing

Schlink, U., O. Herbarth, et al. (2006). "Statistical models to assess the health effects and to forecast ground-level ozone." Environmental Modelling & Software 21(4): 547-558.

SEPP (1999). State Environment Protection Policy (Ambient Air Quality). S19. EPA. Victoria, Australia, Victorian Government Gazette.

Thompson, M. L., J. Reynolds, et al. (2001). "A review of statistical methods for the meteorological adjustment of tropospheric ozone." Atmospheric Environment 35(3): 617-630.

Uppala, S., D. Dee, et al. (2008). Towards a climate data assimilation system: Status update of ERAInterim. ECMWF Newsletter: 12-18.

USEPA (2009). Assessment of the Impacts of Global Change on Regional U.S. Air Quality: A Synthesis of Climate Change Impacts on Ground-Level Ozone. U. S. E. P. Agency. Washington, DC.

WHO (2006). Air Quality Guidelines - Global Update 2005. W. H. Organization. Geneva, WHO Press.

Wise, E. K. and A. C. Comrie (2005). "Meteorologically adjusted urban air quality trends in the Southwestern United States." Atmospheric Environment 39(16): 2969-2980.

Wood, S. (2006). Generalized Additive Models - An Introduction with R. London, Chapman and Hall.

Table 1

Variable	Units	Mean	Median	Min	Max	SD	Definition
O_3	ppb	21.8	21	4	102	9.5	Daily 8-hr Max
PM_{10}	$\mu g/m^3$	17.2	15.6	2	279.7	8.2	Daily Avg
NO_2	ppb	18.4	19	4	90	12	Daily 1-hr Max
Temperature	°C	20	18.9	8.6	44.6	6.3	Daily Max
Sea level pressure	hPa	1017.2	1017.4	991.5	1038.8	7.3	Daily Avg
Global radiation	MJ/m^2	15.3	13.3	0.1	36.6	8.8	Daily Sum
Vapour Pressure	hPa	10.8	10.3	4.6	24.5	2.6	Daily Avg
Zonal (u) wind	km/hr	-4.3	-2.7	-33.2	13.6	6.8	Daily Avg (N+,S-)
Meridonal (v) wind	km/hr	3.7	1.4	-30.6	51.9	15.6	Daily Avg (E+,W-)
Precipitation	mm	1.3	0	0	138.8	5	Daily Sum
Boundary Layer Height	m	1433	1343	195	4937	618.8	4 p.m. LST
Long-term Trend	Days	--	--	1	2922	--	values from 1:2922
Day of week	Days	--	--	0	6	--	values from 0:6
x coordinate	dd.ddd	144.97	--	144.57	145.33	--	Longitude
y coordinate	dd.ddd	-37.84	--	-37.99	-37.71	--	Latitude

Figure 1

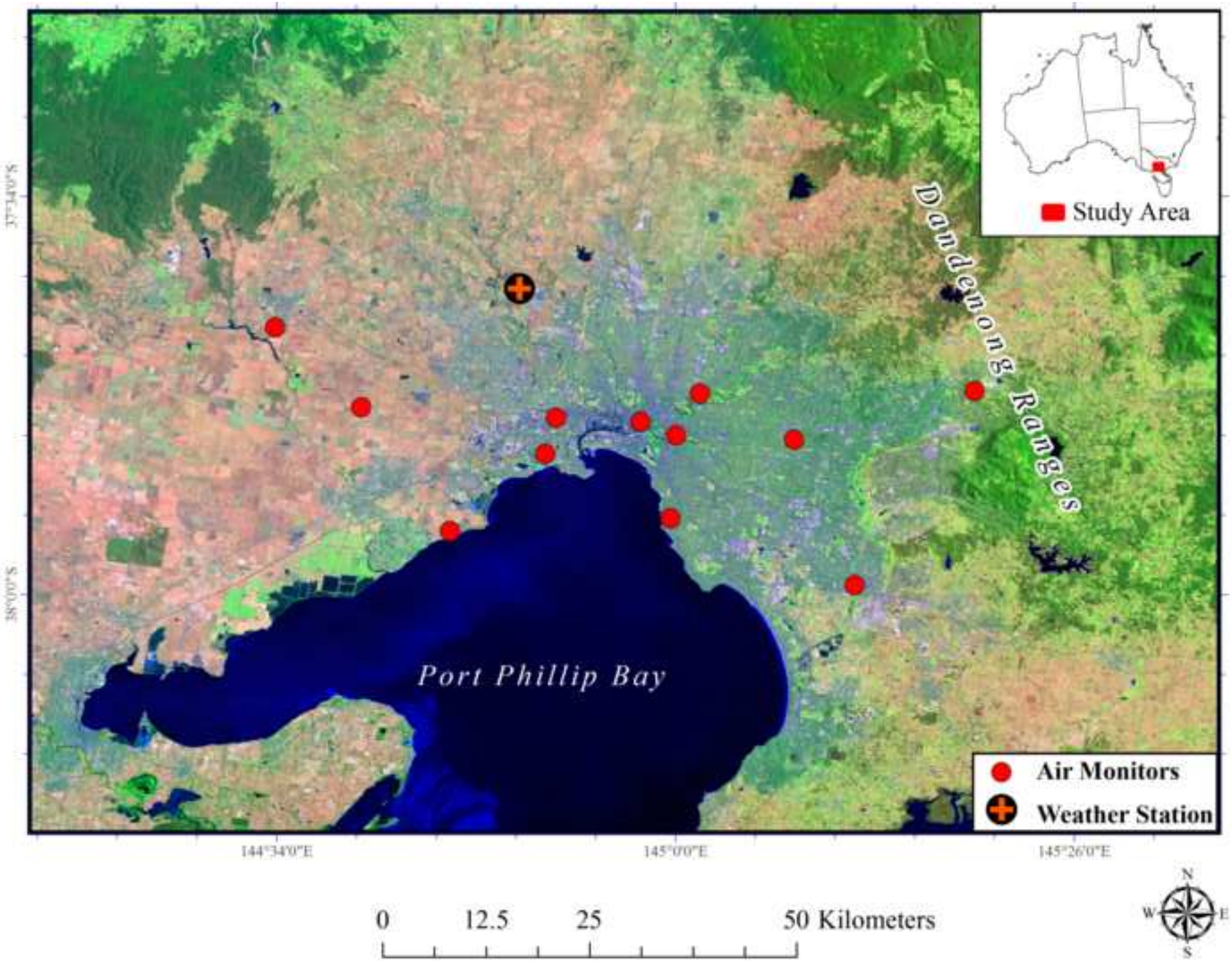
Study Area
Dandenong Ranges
Port Phillip Bay
Air Monitors
Weather Station
144°34'0"E
145°0'0"E
145°26'0"E
0
12.5
25
50 Kilometers
N
W
E
S

Figure 2

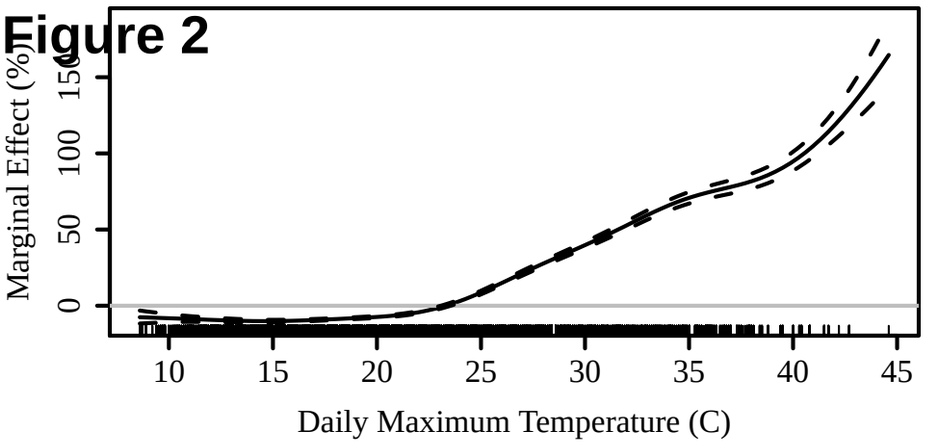
Marginal Effect (%)
0
50
100
150
10
15
20
25
30
35
40
45
Daily Maximum Temperature (C)

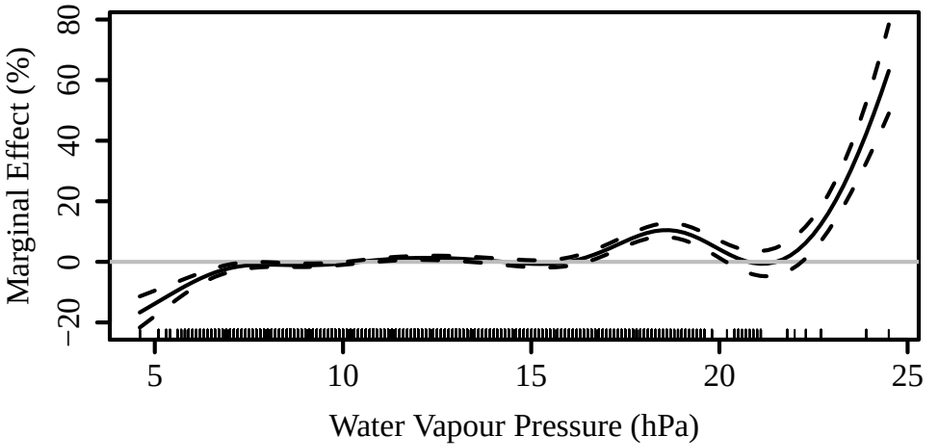
Marginal Effect (%)
−20
0
20
40
60
80
5
10
15
20
25
Water Vapour Pressure (hPa)

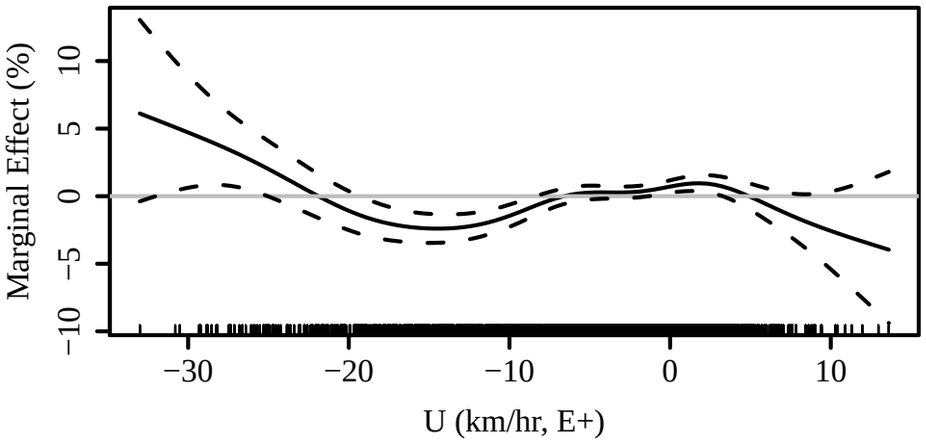
Marginal Effect (%)
−10
−5
0
5
10
−30
−20
−10
0
10
U (km/hr, E+)

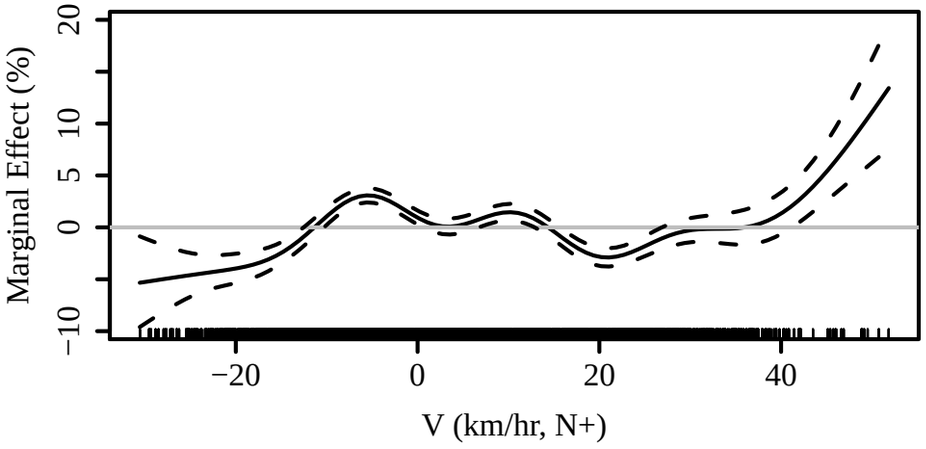
Marginal Effect (%)
−10
0
5
10
20
−20
0
20
40
V (km/hr, N+)

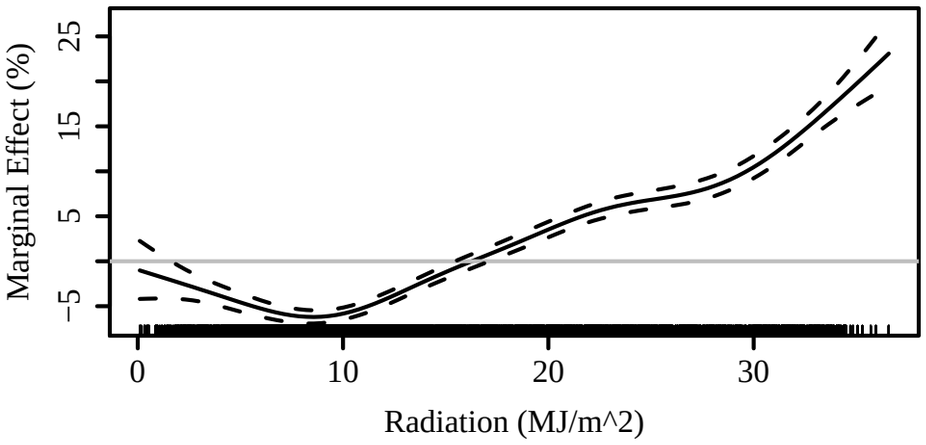
Marginal Effect (%)
−5
5
15
25
0
10
20
30
Radiation (MJ/m^2)

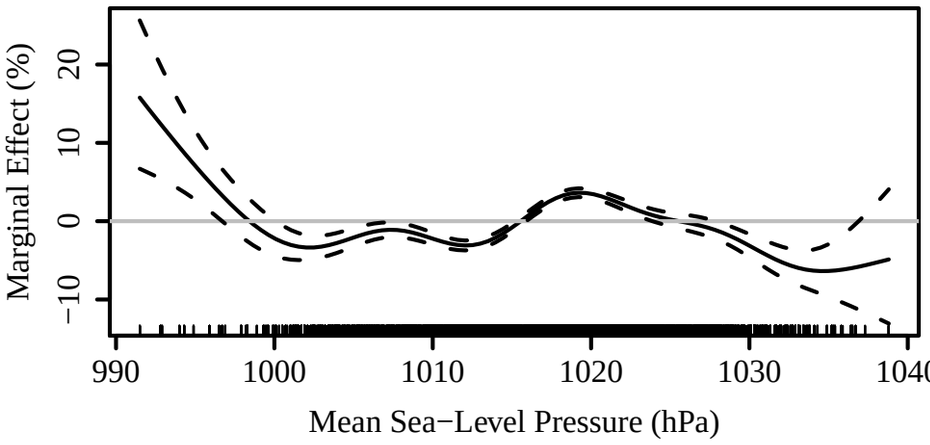
Marginal Effect (%)
−10
0
10
20
990
1000
1010
1020
1030
1040
Mean Sea−Level Pressure (hPa)

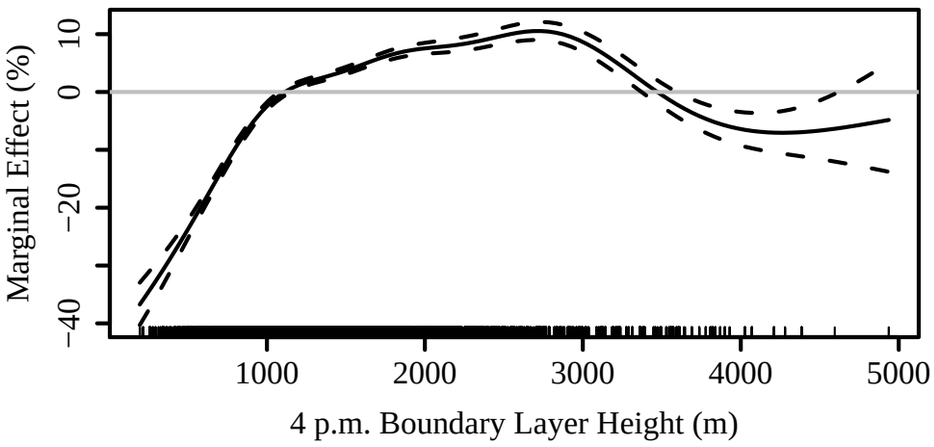
Marginal Effect (%)
−40
−20
0
10
1000
2000
3000
4000
5000
4 p.m. Boundary Layer Height (m)

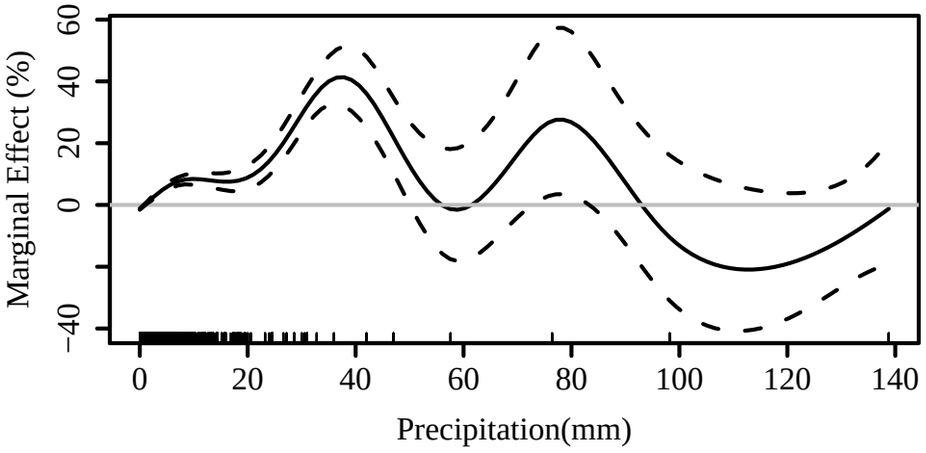
Marginal Effect (%)
−40
0
20
40
60
0
20
40
60
80
100
120
140
Precipitation(mm)

Figure 3

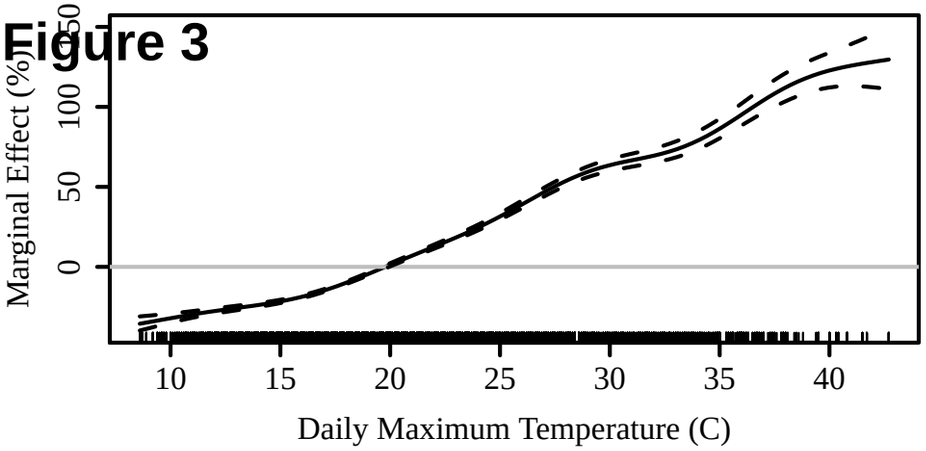
Marginal Effect (%)
0
50
100
150
10
15
20
25
30
35
40
Daily Maximum Temperature (C)

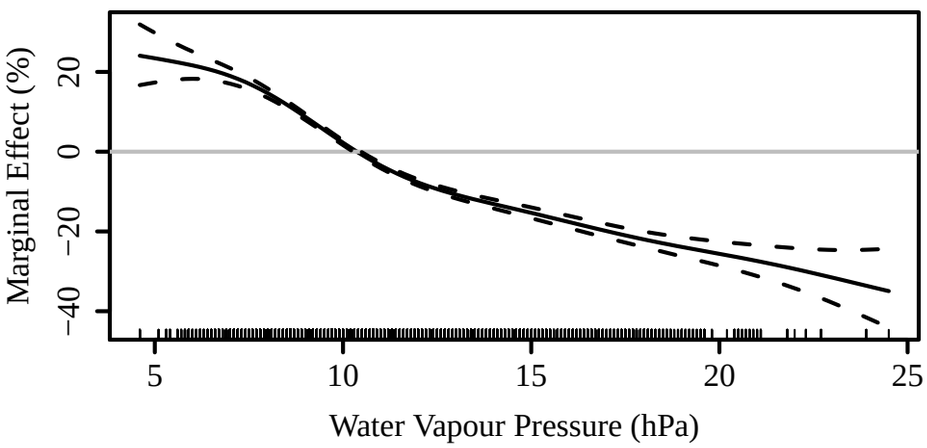
Marginal Effect (%)
−40
−20
0
20
5
10
15
20
25
Water Vapour Pressure (hPa)

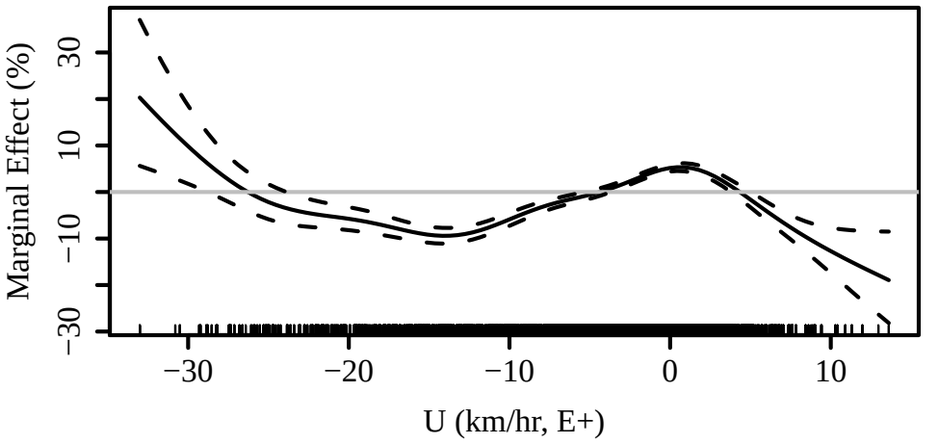
Marginal Effect (%)
−30
−10
10
30
−30
−20
−10
0
10
U (km/hr, E+)

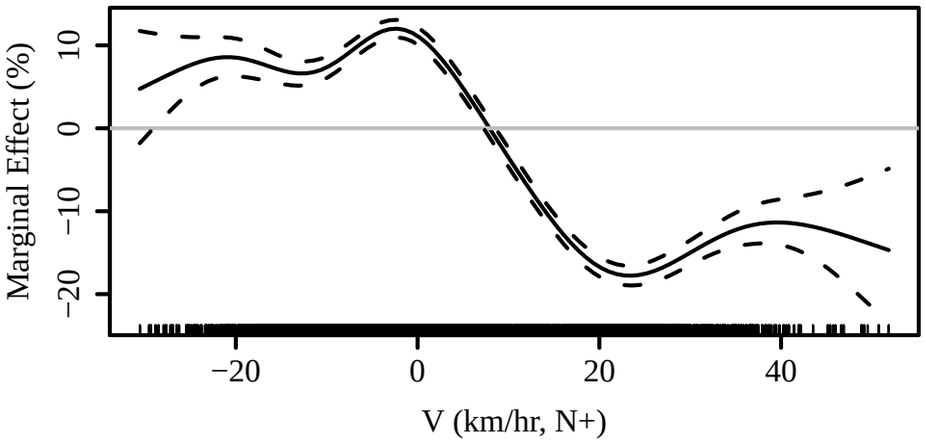
Marginal Effect (%)
−20
−10
0
10
−20
0
20
40
V (km/hr, N+)

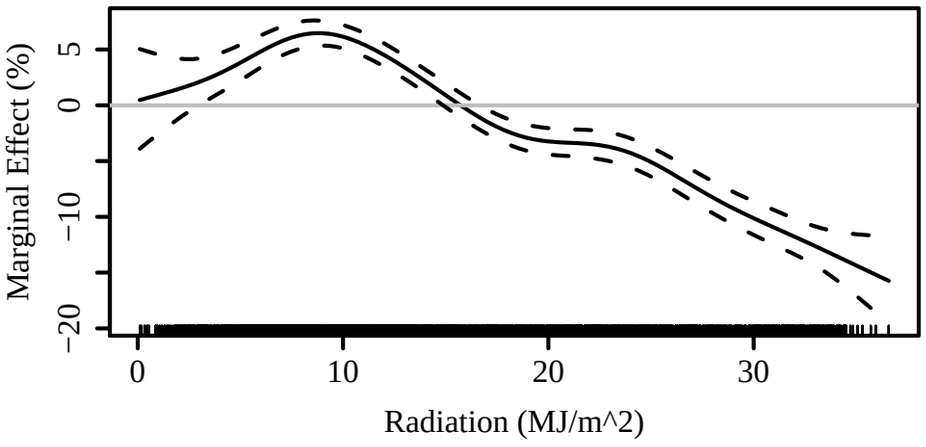
Marginal Effect (%)
−20
−10
0
5
0
10
20
30
Radiation (MJ/m^2)

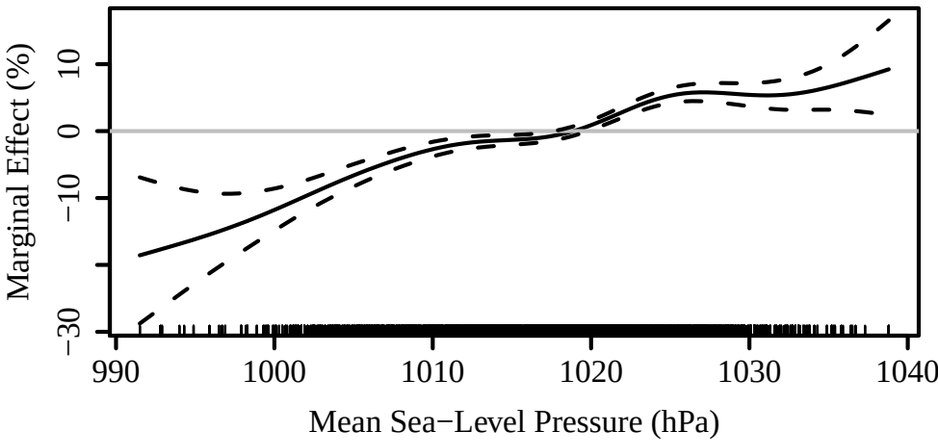
Marginal Effect (%)
−30
−10
0
10
990
1000
1010
1020
1030
1040
Mean Sea−Level Pressure (hPa)

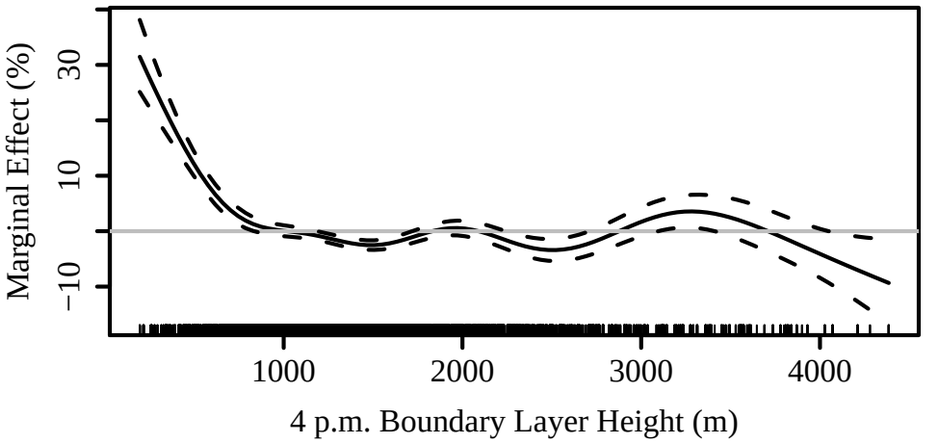
Marginal Effect (%)
−10
10
30
1000
2000
3000
4000
4 p.m. Boundary Layer Height (m)

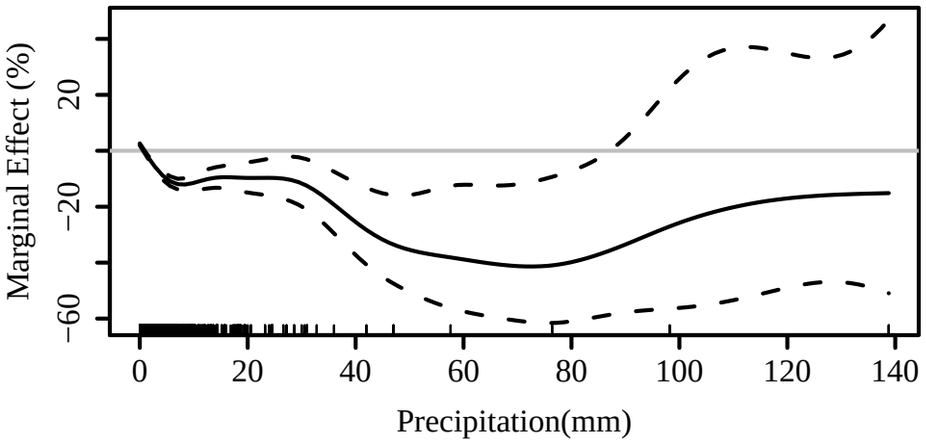
Marginal Effect (%)
−60
−20
20
0
20
40
60
80
100
120
140
Precipitation(mm)

Figure 4

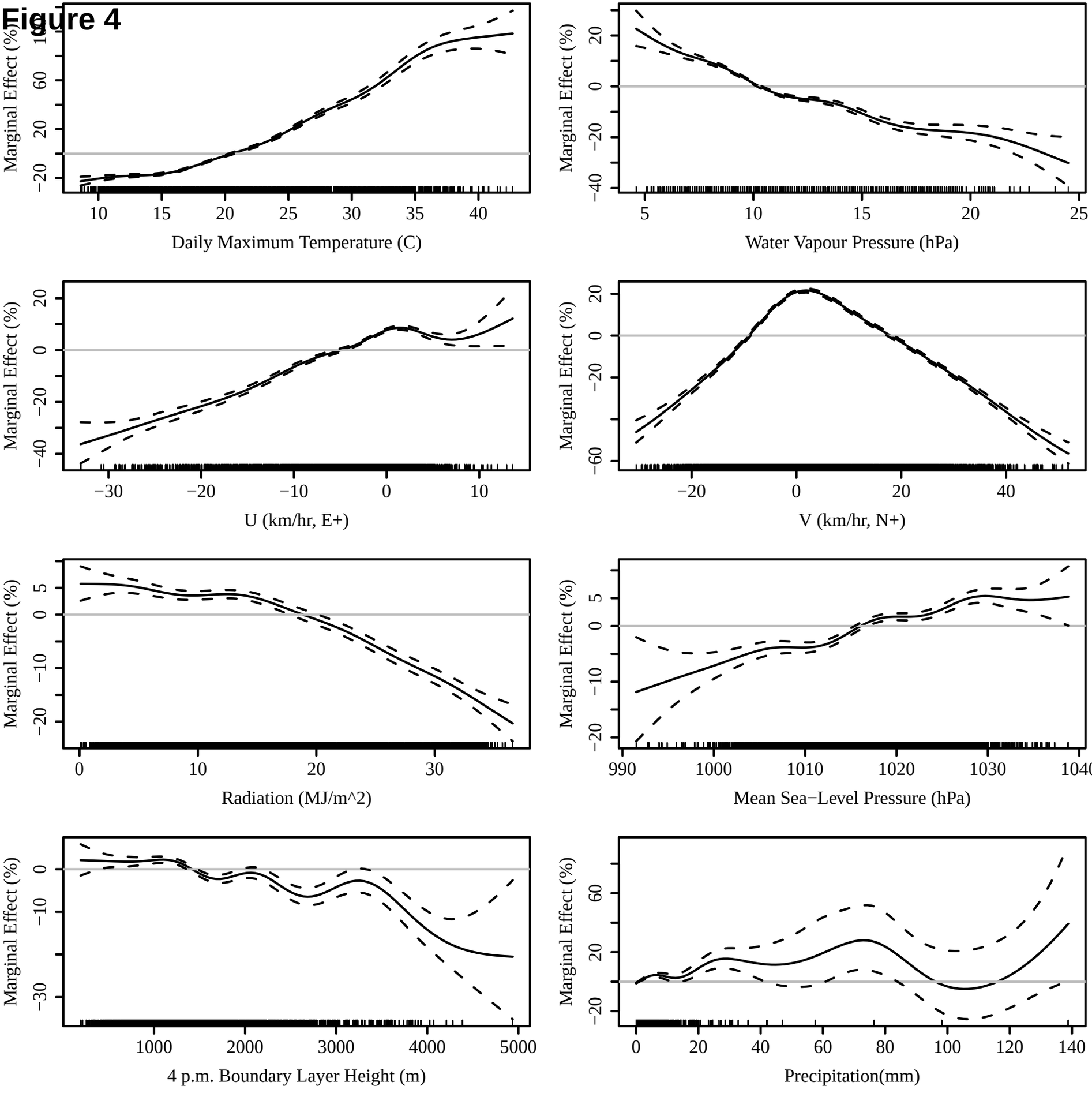
Marginal Effect (%)
Daily Maximum Temperature (C)
Water Vapour Pressure (hPa)
U (km/hr, E+)
V (km/hr, N+)
Radiation (MJ/m^2)
Mean Sea−Level Pressure (hPa)
4 p.m. Boundary Layer Height (m)
Precipitation(mm)